1540 *Chem. Mater.* **2010,** *22,* 1540–1544
DOI:10.1021/cm902882s

CHEMISTRY OF MATERIALS
Article

Novel Cobalt-Free Oxygen-Permeable Perovskite-Type Membrane

Konstantin Efimov,* Torben Halfer, Alexander Kuhn, Paul Heitjans, Jürgen Caro, and Armin Feldhoff

Institute of Physical Chemistry and Electrochemistry, and Center for Solid State Chemistry and New Materials, Leibniz Universität Hannover, Callinstrasse 3-3A, 30167 Hannover, Germany

Received September 15, 2009. Revised Manuscript Received December 9, 2009

Cobalt-free perovskite with the novel composition $(Ba_{0.5}Sr_{0.5})(Fe_{0.8}Cu_{0.2})O_{3-\delta}$ (BSFCu) was synthesized via a sol−gel method and studied with respect to the crystallographic structure as well as the oxygen ionic and the electronic conductivity. In situ X-ray diffraction (XRD) was applied to investigate the thermal dilatation and the phase stability of the BSFCu at high and intermediate temperatures. Additionally, time-dependent oxygen permeation performance measurements were carried out for BSFCu and Co-based $(Ba_{0.5}Sr_{0.5})(Co_{0.8}Fe_{0.2})O_{3-\delta}$ membranes at 1023 K for 200 h. The BSFCu phase was found to be a cubic perovskite by XRD and transmission electron microscopy. The BSFCu membrane exhibits a very high oxygen permeation and electrical conductivity as compared to known perovskite membranes. The oxygen permeation of the BSFCu membrane maintains its value for 200 h at 1023 K unlike $(Ba_{0.5}Sr_{0.5})(Co_{0.8}Fe_{0.2})O_{3-\delta}$, whose oxygen flux was reduced by one-half during the same interval.

Introduction

For many fields of application as cathode in solid-oxide fuel cells (SOFCs), in the production of oxygen-enriched air, and in the conversion of hydrocarbons to synthesis gas,[1−3] mixed ionic−electronic conductors (MIECs) are on the verge of a breakthrough. Nevertheless, membrane materials with improved qualities for industrial processes are needed. Cobalt-based perovskite oxides like $(La_xSr_{1-x})(Co_yFe_{1-y})O_{3-\delta}$ or $(Ba_xSr_{1-x})(Co_yFe_{1-y})O_{3-\delta}$ are often thought to be the most promising materials because they show very good oxygen permeability due to the extremely high amount of disordered oxygen vacancies and their excellent phase stability above 1173 K.[4,5] The flexible redox behavior of cobalt, however, leads to two considerable disadvantages. First, the large coefficient of thermal expansion (CTE) of cobaltites, with values between 20 and 24 $\times$ 10^{-6} K^{-1} over a wide temperature range,[6,7] is responsible for huge thermal stresses and can result in cracking of the ceramic products during operation in the worst case. Second, the cubic structure of Co-based perovskites at intermediate temperatures (IT, approximately $T = 773-1073$ K) breaks down under long-term conditions.[5,8−10] The driving force for this conversion is a temperature-dependent coupled valence and spin-state transition of cobalt (between high spin Co^{2+} and low spin Co^{3+}). The small ionic radius of trivalent cobalt in low-spin configuration favors the formation of the hexagonal perovskite phase.[11,12] This fact excludes cobaltites from use as membrane materials in the IT range. Thus, the development of Co-free perovskite systems is of large and persistent interest.

Due to the less flexible redox behavior of iron, Fe-based perovskite oxides attracted much attention as possible alternatives to cobaltites in the past few years. Teraoka et al.[13] and Zhen et al.[14] reported that $Ba_xSr_{1-x}FeO_{3-\delta}$ systems reveal a high oxygen permeation flux accompanied with an exceedingly high phase stability. Furthermore, Wang et al.[15] and Martynczuk et al.[16] established an increase of the oxygen permeation rate by substituting $(Ba_xSr_{1-x})FeO_{3-\delta}$ with lower valence cations like Zn^{2+} and Al^{3+} for the B-site of the perovskite. Continuing the research on Co-free perovskite systems, we have

*Corresponding author. E-mail: konstantin.efimov@pci.uni-hannover.de.

(1) Shao, Z.; Haile, S. M. *Nature* **2004**, *431*, 170.
(2) Wang, H.; Werth, S.; Schiestel, T.; Caro, J. *Angew. Chem., Int. Ed.* **2005**, *44*, 6906.
(3) Chen, C.; Feng, S.; Ran, S.; Zhu, D.; Liu, W.; Bouwmeester, H. J. M. *Angew. Chem., Int. Ed.* **2003**, *115*, 5196.
(4) Teraoka, Y.; Zhang, H.; Furukawa, S.; Yamazoe, N. *Chem. Lett.* **1985**, *11*, 1743.
(5) Shao, Z.; Yang, W.; Cong, Y.; Dong, H.; Tong, J.; Xiong, G. *J. Membr. Sci.* **2000**, *172*, 177.
(6) McIntosh, S.; Vente, J. F.; Haije, W. G.; Blank, D. H. A.; Bouwmeester, H. J. M. *Chem. Mater.* **2006**, *18*, 2187.
(7) Vente, J. F.; Haije, W. G.; Rak, Z. S. *J. Membr. Sci.* **2006**, *177*, 2245.
(8) Švarcová, S.; Wiik, K.; Tolchard, J.; Bouwmeester, H. J. M.; Grande, T. *Solid State Ionics* **2008**, *178*, 1787.
(9) Teraoka, Y.; Nobunaga, T.; Namazoe, Y. *Chem. Lett.* **1988**, *3*, 503.
(10) Nagai, T.; Ito, W.; Sakon, T. *Solid State Ionics* **2007**, *177*, 3433.
(11) Arnold, M.; Gesing, T. M.; Martynczuk, J.; Feldhoff, A. *Chem. Mater.* **2008**, *20*, 5881.
(12) Arnold, M.; Xu, Q.; Tichelaar, F. D.; Feldhoff, A. *Chem. Mater.* **2009**, *21*, 635.
(13) Teraoka, Y.; Shimokawa, H.; Kang, C. Y.; Kusaba, H.; Sasaki, K. *Solid State Ionics* **2006**, *177*, 2245.
(14) Chen, Z.; Ran, R.; Zhou, W.; Shao, Z.; Liu, S. *Electrochim. Acta* **2007**, *52*, 7343.
(15) Wang, H.; Tablet, C.; Feldhoff, A.; Caro, J. *Adv. Mater.* **2005**, *17*, 1785.
(16) Martynczuk, J.; Liang, F.; Arnold, M.; Šepelák, V.; Feldhoff, A. *Chem. Mater.* **2009**, *21*, 1586.

 Published on Web 01/08/2010

developed a Cu-doped perovskite with the novel composition $(Ba_{0.5}Sr_{0.5})(Fe_{0.8}Cu_{0.2})O_{3-\delta}$ (BSFCu), which is the focus of this paper. The Fe ion normally takes a mixed oxidation state between 3+ and 4+ in perovskite oxides.[16,17] Replacing of Fe ions with divalent and trivalent Cu ions[18] in a perovskite lattice can lead to an increase of oxygen vacancies, from which one would expect to observe improved oxygen-conducting behavior. Already in 1988 and 1991, Teraoka et al. have shown the positive effect of Cu-doping on the $(La_xSr_{1-x})CoO_{3-\delta}$ oxygen permeability.[9,19] Similarly, Cu-containing $Sr(Fe_xCu_{1-x})O_{3-\delta}$ perovskites with a high oxygen conductivity are reported in the literature.[20,21] Because $SrFeO_{3-\delta}$-based perovskite oxides tend to form a brownmillerite phase like $Sr_2Fe_2O_5$, their large-scale application would be inhibited.[20,22]

Experimental Section

A sol−gel route using metal nitrates, citrate, and ethylenediaminetetraacetic acid (EDTA) as described in detail elsewhere[23−25] was applied to prepare the BSFCu material. A powder obtained after heat treatment for 10 h at 1223 K was uniaxially pressed under 140−150 kN for 20 min into green bodies. The pellets were calcined for 10 h at 1323 K with a heating and cooling rate of 3 K/min to form dense membrane disks with a diameter of 16 mm and a thickness of 1.1 mm.

The XRD was carried out in a Θ/2Θ geometry on a Philips X'pert-MPD instrument using Cu Kα radiation at 40 kV and 40 mA, with a receiving slit of 0.05 mm. For Pawley refinement, the data were collected in a 2Θ range of 15°-90° in a step-scan mode with a step width of 0.04° and count time of 25 s per step. The Pawley refinement was performed by using Topas V4.1 software (Coehlo Software). During in situ high-temperature XRD measurements, data were collected in 2Θ ranges of 30°-33° and 20°-60° with intervals of 0.02° and count times of 33 s/step and 5 s/step, respectively. The tests were conducted in a high temperature cell (HDK 2.4 with REP 2000) with Pt−Rh holder in the temperature range of 308−1173 K in steps of 100 K with a heating and cooling rate of 3 K/min in air. Before each data acquisition, an equilibration time of 30 min was used.

Scanning electron microscopy (SEM) imaging was performed on a JEOL JSM-6700F field-emission instrument at a low excitation voltage of 2 kV. An energy-dispersive X-ray spectrometer (EDXS), Oxford Instruments INCA-300, with an ultrathin window was used for the elemental analysis at an excitation voltage of 15 kV.

Transmission electron microscopy (TEM) investigations were made at 200 kV on a JEOL JEM-2100F-UHR field-emission instrument (C_S = 0.5 mm, C_C = 1.2 mm). The microscope was operated as a high-resolution TEM (HRTEM) as well as a scanning TEM (STEM) in bright-field mode. The preparation method of the TEM specimen is described in detail elsewhere.[26] Additionally, HRTEM micrographs were simulated by using the electron microscopy software JEMS (Java version V3-3526U2008 s, P. Stadelmann, CIME-EPFL).

Conductivity measurements by impedance spectroscopy were performed using a four terminal configuration in the temperature range from room temperature to 1173 K with a heating rate of about 10 K/min in air. Pellets of about 1 mm thickness were prepared by room temperature pressing and subsequent sintering. Long sticks were cut from the pellet to enable low impedance measurements. Silver conductive paste was used as electrode material. The frequency dependence of the conductivity was negligible in the frequency range from 10 Hz to 100 kHz. Data shown here were recorded at a frequency of 50 Hz using a HP 4192 A impedance analyzer. The setup including the sample holder is described in detail elsewhere.[27]

Oxygen permeation was measured in a high-temperature permeation cell[28] according to the method described elsewhere.[29] Air was fed at a rate of 150 mL min^{-1} to the feed side; He (29.0 mL min^{-1}, 99.995%) and Ne (1.0 mL min^{-1}, 99.995%) gases were fed to the sweep side. The effluents were analyzed by gas chromatography on an Agilent 6890 instrument equipped with a Carboxen 1000 column. The gas concentrations in the effluent stream were calculated from a gas chromatograph calibration. The absolute flux rate of the effluents was determined by using neon as an internal standard. The relative leakage of O_2, which was evaluated by measuring the amount of N_2 in the effluent stream, was subtracted in the calculation of the oxygen permeation flux.

Results and Discussion

The stoichiometric $(Ba_{0.5}Sr_{0.5})(Fe_{0.8}Cu_{0.2})O_{3-\delta}$ perovskite oxide was synthesized via a sol−gel method, which affords a fine intermixing of the cations during all processing steps, thus leading to a pure product phase at comparably low synthesis temperatures and dwell times. Figure 1 displays an XRD pattern of the BSFCu powder. The desired product was found to be a pure perovskite phase. The cubic symmetry in the $Pm\bar{3}m$ space group (Nr. 221) with a = 3.9434(4) Å (lattice parameter) was determined by Pawley-analysis.[30] The refinement converged to reliability factors of R_{WP} = 11.162, R_{SP} = 8.91 and to a goodness of the fit of 1.253. Obviously, Cu ions ($r(Cu^{2+})$ = 0.73 Å, $r(Cu^{3+})$ = 0.54 Å)[31] can be incorporated at the B-position of the ABO_3 perovskite (A: $r(Ba^{2+})$ = 1.61 Å, $r(Sr^{2+})$ = 1.44 Å, B: $r(Fe^{3+}$, high spin) = 0.645 Å, $r(Fe^{4+}$, high spin) = 0.585 Å, $r(O^{2-})$ = 1.40 Å)[31]

(17) Feldhoff, A.; Martynczuk, J.; Arnold, M.; Myndyk, M.; Bergmann, I.; Šepelák, V.; Gruner, W.; Vogt, U.; Hähnel, A.; Woltersdorf, J. *J. Solid State Chem.* **2009**, *182*, 2961.
(18) Bringley, J. F.; Scott, B. A.; Laplaca, S. J.; Boehme, R. F.; Shaw, T. M.; McElfresh, M. W.; Trail, S. S.; Cox, D. E. *Nature* **1990**, *347*, 263.
(19) Teraoka, Y.; Nobunaga, T.; Okamoto, K.; Miura, N.; Yamazoe, N. *Solid State Ionics* **1991**, *48*, 207.
(20) Zhang, H.; Wang, T.; Dong, X.; Lin, W. *J. Nat. Gas Chem.* **2009**, *18*, 45.
(21) Nie, H.; Zhang, H.; Yu, G.; Yang, N. *Sep. Pur. Technol.* **2001**, *25*, 415.
(22) McIntosh, S.; Vente, J. F.; Haije, W. G.; Blank, D. H. A.; Bouwmeester, H. J. M. *Solid State Ionics* **2006**, *177*, 833.
(23) Martynczuk, J.; Arnold, M.; Caro, J.; Wang, H.; Feldhoff, A. *Adv. Mater.* **2007**, *19*, 2134.
(24) Feldhoff, A.; Arnold, M.; Martynczuk, J.; Gesing, T. M.; Wang, H. *Solid State Sci.* **2008**, *10*, 689.
(25) Feldhoff, A.; Martynczuk, J.; Wang, H. *Prog. Solid State Chem.* **2007**, *35*, 339.
(26) Arnold, M.; Wang, H.; Feldhoff, A. *J. Membr. Sci.* **2007**, *293*, 44.
(27) Indris, S.; Heitjans, P.; Roman, H. E.; Bunde, A. *Phys. Rev. Lett.*, **2000**, *84*, 2889; S. Indris, Thesis, University of Hannover, Germany, **2001**.
(28) Wang, H.; Tablet, C.; Feldhoff, A.; Caro, J. *J. Membr. Sci.* **2005**, *262*, 20.
(29) Martynczuk, J.; Arnold, M.; Feldhoff, A. *J. Membr. Sci.* **2008**, *322*, 375.
(30) Pawley, G. S. *J. Appl. Crystallogr.* **1981**, *14*, 357.
(31) Shannon, R. D. *Acta Crystallogr., Sect. A: Found. Crystallogr.* **1976**, *32*, 751.

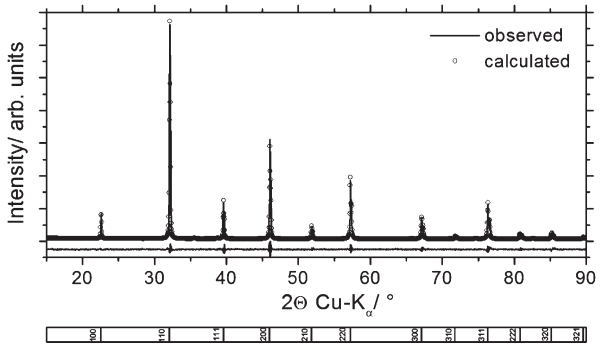

Figure 1. XRD pattern of BSFCu: observed, calculated by the Pawley method, and difference (bottom line). The calculated Bragg positions are marked with ticks at the bottom of the figure.

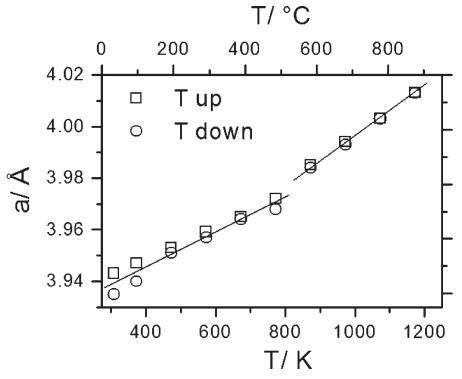

Figure 2. Lattice parameter of BSFCu as a function of the temperature during heating and cooling.

without distorting the cubic structure. This is in agreement with Goldschmidt's tolerance factor of BSFCu calculated to be in the range of $t = 1.003-1.046$ for various ratios of Fe^{4+}/Fe^{3+} ions and Cu^{3+}/Cu^{2+} ions. Therefore, the cubic space group $Pm3\overline{m}$ was expected for BSFCu because the tolerance factor lies close to unity, which is a benchmark for cubic symmetry.[32]

In order to examine the behavior of the BSFCu powder at high temperatures, in situ XRD experiments were carried out in the temperature range of 308−1173 K with steps of 100 K under ambient air. Confirmed by measurements in the angle interval 20°-60° 2Θ, the cubic perovskite was found to be stable in the entire temperature range, since no reflexes of other phases appeared. The shift of the lattice parameters with temperature was derived in particular from the (110) reflex of the cubic structure in the 30°-33° 2Θ range. Figure 2 shows the change of the lattice parameter, determined from the 2Θ angular position of the peak under consideration, during heating and cooling. From these measurements, the CTE of BSFCu could be estimated to be approximately $16 \times 10^{-6}\ K^{-1}$ between room temperature and 773 K as well as approximately $23 \times 10^{-6}\ K^{-1}$ between 773 and 1173 K. Thus, the CTE of BSFCu gives a lower dilatation in the IT range and a similar dilatation at high temperatures compared to the CTE values of cobaltites reported by McIntosh et al.,[6] Vente et al.,[7] and Wei et al.[33]

(32) Goldschmidt, V. M. *Naturwissenschaften* **1926**, *14*, 477.
(33) Wei, B.; Lu, Z.; Huang, X.; Miao, J.; Sha, X.; Xin, X.; Su, W. *J. Eur. Ceram. Soc.* **2006**, *26*, 2827.

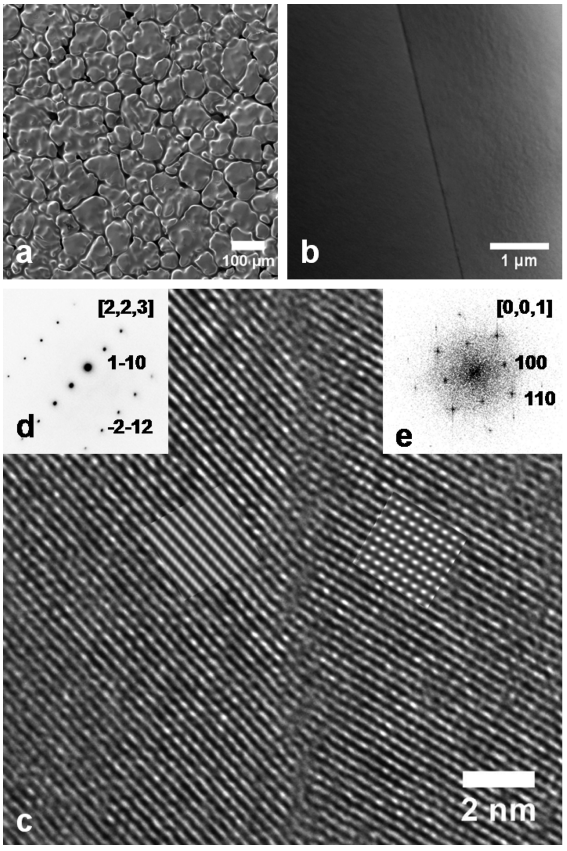

Figure 3. a) SEM of the BSFCu membrane surface. b) STEM and c) HRTEM showing an interface of two BSFCu perovskite grains. Insets show images calculated with −32 nm defocus for [2,2,3] and [0,0,1] zone axis for BSFCu, respectively. d) Selected area diffraction of the grain on the left in Figure 3c. e) Two-dimensional fast Fourier transformed from the grain on the right in Figure 3c.

After sintering, the BSFCu ceramic was investigated by electron microscopy. The SEM micrograph in Figure 3a shows the surface of the membrane. No cracks and only a few pores are visible on the membrane surface. The pores are not running throughout the membrane as evidenced by SEM of the cross-section. To verify the chemical composition of the membrane, EDX spectra were acquired from the surface and the cross-section. A Cliff-Lorimer quantification of the EDX spectra confirmed the desired $(Ba_{0.5}Sr_{0.5})(Fe_{0.8}Cu_{0.2})O_{3-\delta}$ stoichiometry. Furthermore, the BSFCu ceramic strikes by large grains with an average size of about 100 μm. The grain size distribution and the nature of the grain boundaries might be key factors in the oxygen permeation performance. The bright-field STEM micrograph and HRTEM micrograph in Figure 3b and Figure 3c, respectively, present the grain boundary between two perovskite grains revealed by selected area electron diffraction (SAED) (Figure 3d) or due to two-dimensional fast Fourier transformation (FFT) (Figure 3e). Both perovskite grains are in close contact. No amorphous phase, or any other substance, was observed at the interface. The grain on the left-hand side is oriented along the zone axis [2,2,3], and the grain on the right-hand side is oriented along the zone axis [0,0,1]. Additionally, the HRTEM micrograph in Figure 3c was extended by contrast simulations

Table 1. Comparison of Oxygen Permeation Flux Through Several Related Perovskite Membranes

	oxygen permeation flux/mL cm^{-2} min^{-1}		
perovskite membranes	1023 K	1223 K	E_A/kJ mol^{-1}
$(Ba_{0.5}Sr_{0.5})(Fe_{0.8}Zn_{0.2})O_{3-\delta}$	0.36	0.98	55
$(Ba_{0.5}Sr_{0.5})(Fe_{0.9}Al_{0.1})O_{3-\delta}$[16]	0.41[a]	1.19	44
$(Ba_{0.5}Sr_{0.5})(Fe_{0.8}Cu_{0.2})O_{3-\delta}$	0.53	1.60	47
$(Ba_{0.5}Sr_{0.5})(Co_{0.8}Fe_{0.2})O_{3-\delta}$	1.31	2.66	46

[a] Value is extrapolated with the assumption of a linear progress of the oxygen permeation flux depending on the temperature.

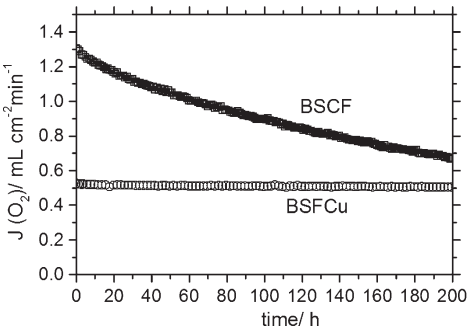

Figure 4. Oxygen permeation flux through $(Ba_{0.5}Sr_{0.5})(Fe_{0.8}Cu_{0.2})O_{3-\delta}$ (BSFCu) and $(Ba_{0.5}Sr_{0.5})(Co_{0.8}Fe_{0.2})O_{3-\delta}$ (BSCF) membranes as a function of time at 1023 K.

performed via JEMS software for each grain according to its orientation, which show good correlation with experimental results.

In order to be a candidate for a promising membrane material, a novel perovskite system must show a good oxygen permeation performance. Because the value of oxygen flux through a membrane strongly depends on the experimental conditions, such as the membrane thickness and oxygen partial pressures on the permeate and the feed side, it is problematic to compare the detected oxygen permeation flux with data given in the literature. Table 1 summarizes the results of oxygen permeation measurements of several related perovskite membranes of equal thickness (1.1 mm) conducted under the same conditions. Thus, it appears that the oxygen flux through the BSFCu membrane, both at intermediate (1023 K) and at high temperatures (1223 K), is significantly higher than the flux through $(Ba_{0.5}Sr_{0.5})(Fe_{0.8}Zn_{0.2})O_{3-\delta}$ and $(Ba_{0.5}Sr_{0.5})(Fe_{0.9}Al_{0.1})O_{3-\delta}$ membranes. The permeation flux of $(Ba_{0.5}Sr_{0.5})(Co_{0.8}Fe_{0.2})O_{3-\delta}$, however, remains unrivalled. The activation energies were calculated from the temperature dependence of the oxygen permeation as given in Table 1.

For perspective application in the IT range, the most important factor for perovskite materials is a constant oxygen permeation performance owing to phase stability in addition to good mixed oxygen-ionic and electronic conductivity. For this reason, time-dependent oxygen permeation experiments were carried out for BSFCu and the prominent $(Ba_{0.5}Sr_{0.5})(Co_{0.8}Fe_{0.2})O_{3-\delta}$ perovskite in the IT range. Figure 4 shows the oxygen permeation flux through both membranes at 1023 K. The oxygen permeation of the BSFCu membrane maintains a value of

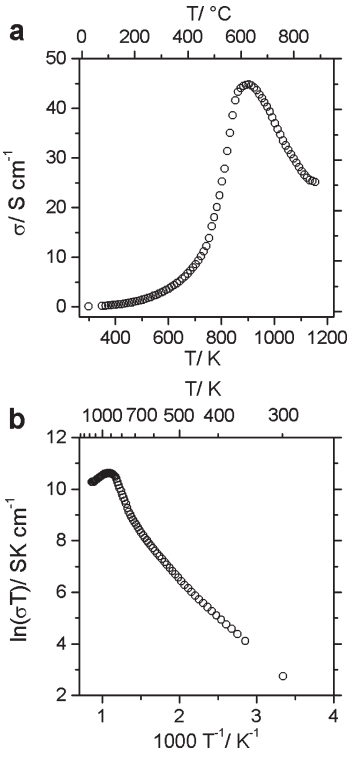

Figure 5. Electrical conductivity of BSFCu pellet: a) σ as a function of temperature and b) σT in Arrhenius representation.

0.53 mL cm^{-2} min^{-1} for more than 200 h. The flux through the $(Ba_{0.5}Sr_{0.5})(Co_{0.8}Fe_{0.2})O_{3-\delta}$ membrane continuously decreases with time. The flux was reduced by one-half after 200 h, from 1.31 mL cm^{-2} min^{-1} to 0.66 mL cm^{2-} min^{-1}, which was caused by the intrinsic phase instability of the $(Ba_{0.5}Sr_{0.5})(Co_{0.8}Fe_{0.2})O_{3-\delta}$ perovskite at intermediate temperatures[5,8−12]. After the measurement, the microstructure of the BSFCu material was analyzed by SEM, EDXS, and XRD. SEM investigations combined with EDXS of the feed side, the permeate side, and the cross-section of the membrane exhibit the absence of cracks and coats in the ceramic. With the help of XRD, the BSFCu material was proved to maintain its cubic perovskite structure as a single pure phase during the performance test at 1023 K for 200 h. Thus, these results show the advantage of the BSFCu perovskite over $(Ba_{0.5}Sr_{0.5})(Co_{0.8}Fe_{0.2})O_{3-\delta}$ materials for operation in the IT range.

The total electrical conductivity of the BSFCu ceramic was studied via the four-point probe method at ambient air. As demonstrated in Figure 5a, the conductivity increases with increasing temperature and reaches a maximum value of 45 S cm^{-1} at around 890 K. This semiconducting behavior can be explained by a thermally activated p-type small polaron-hopping mechanism.[34] An activation energy of 23.2 kJ mol^{-1} was determined from the linear part of the Arrhenius plot (Figure 5b) in the temperature range of 300−500 K. The changeover from semiconduction to metallic conduction of the BSFCu above 890 K may be related to a spin-state transition of the Fe ions.[17,35,36] The

(34) Stevenson, J. W.; Armstrong, T. R.; Carneim, R. D.; Pederson, L. R.; Weber, W. J. *J. Electrochem. Soc.* **1996**, *143*, 2722.

total conductivity of BSFCu is comparable with that of $(Ba_{0.5}Sr_{0.5})(Co_{0.8}Fe_{0.2})O_{3-\delta}$, which shows a maximum value of approximately 45−50 S cm^{-1} at about 820 K.[37] The established Co-free material, such as $(Ba_{0.5}Sr_{0.5})(Fe_{0.8}Zn_{0.2})O_{3-\delta}$, shows a lower conductivity with a maximum of 9.4 S cm^{-1} at about 860 K.[38]

(35) Raccah, P. M.; Goodenough, J. B. *Phys. Rev.* **1967**, *155*, 932.
(36) Bhide, V. G.; Rao, G. R.; Rao, C. N. R.; Rajoria, D. S. *Phys. Rev. B* **1972**, *6*, 1021.
(37) Zhao, H.; Shen, W.; Zhu, Z.; Li, X.; Wang, Z. *J. Power Sources* **2008**, *182*, 503.
(38) Wei, B.; Lu, Z.; Huang, X.; Miao, J.; Sha, X.; Xin, X.; Su, W. *J. Power Sources* **2008**, *176*, 1.

Conclusions

The novel cubic perovskite BSFCu was designed to be an alternative to Co-based perovskites. This material exhibits a good phase stability at high and intermediate temperatures and a better oxygen permeation performance as compared to related Fe-based perovskites. With regard to thermal dilatation and electrical conductivity, BSFCu is comparable to $(Ba_{0.5}Sr_{0.5})(Co_{0.8}Fe_{0.2})O_{3-\delta}$. The stability of the BSFCu material during the operation in the IT range clearly exceeds that of $(Ba_{0.5}Sr_{0.5})(Co_{0.8}Fe_{0.2})O_{3-\delta}$.